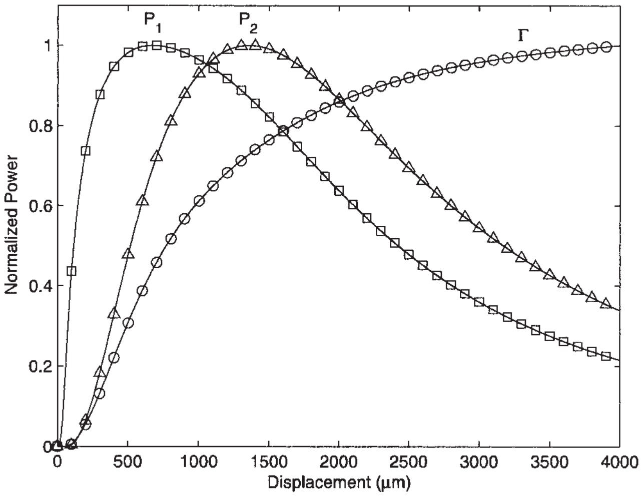

Figure 6 Experimental (□ power from inner RFB, △ power from outer RFB, ○ ratio of powers from two RFBs) and theoretical (—) response curves

power fluctuation and target-reflectivity variation. All the theoretical and experimental results are capable of offering quantitative guidance for the design and implementation of fiber-bundle sensors.

REFERENCES

1. Y. Alayli, S. Topçu, D. Wang, R. Dib, and L. Chassagne, Applications of a high accuracy optical fiber displacement sensor to vibrometry and profilometry, Sens Actuat A 116 (2004), 85–90.
2. H. Golnabi, Design of an optical fiber sensor for linear thermal expansion measurement, Opt Laser Technol 34 (2002), 389–394.
3. J. Park, M. Kim, Y. Kim, K. Kim, and I. Kim, Intensity-based fiber optic pressure sensor with an $Au/NiCr/Si_3N_4/SiO_2/Si_3N_4$ diaphragm, Proc SPIE 3897 (1999), 565–569.
4. G. He and F.W. Cuomo, Displacement response detection limit and dynamic range of fiber-optic lever sensors, J Lightwave Technol 9 (1991), 1618–1625.
5. R.O. Cook and C.W. Hamm, Fiber optic lever displacement transducer, Appl Opt 18 (1979), 3230–3241.
6. A. Shimamoto and K. Tanaka, Geometrical analysis of an optical fiber bundle displacement sensor, Appl Opt 35 (1996), 6767–6774.
7. Z. Zhao, W.S. Lau, A.C.K. Choi, and Y.Y. Shan, Modulation functions of a reflective fiber sensor with random fiber arrangement based on a pair model, Opt Eng 34 (1995), 3055–3061.
8. L. Bergougnoux, J. Misguich-Ripault, and J.-L. Firpo, Characterization of an optical fiber bundle sensor, Rev Sci Instrum 69 (1998), 1985–1990.
9. J.B. Faria, A theoretical analysis of the Bifurcated fiber bundle displacement sensor, IEEE Trans Instrum Meas 47 (1998), 742–747.
10. L. Yuan, J. Pan, T. Yang, and G. Han, Analysis of the compensation mechanism of a fiber-optic displacement sensor, Sens Actuat A 36 (1993), 177–182.
11. J.B. Faria, Modeling the Y-branched optical fiber bundle displacement sensor using a quasi-gaussian beam approach, Microwave Opt Technol Lett 25 (2000), 138–141.
12. Y. Yang, K. Yamazaki, H. Aoyama, and S. Matsumiya, Fiber optical surface topography measurement sensor and its design study, Precis Eng 24 (2000), 32–40.
13. H. Lu, T. Xu, H. Yang, and Z. Chen, Research of a reflective fiber-optic displacement sensor with intensity compensation, Proc SPIE 4222 (2000), 313–317.

DYNAMIC OF THE DEGREE OF POLARIZATION IN A DEPOLARIZING CHANNEL: THEORY AND EXPERIMENTAL RESULTS

José Cláudio do Nascimento and Rubens Viana Ramos
Department of Teleinformatic Engineering
Federal University of Ceará
Campus do Pici
C.P. 6007, 60455-760, Fortaleza-Ceará, Brazil

Received 12 August 2005

ABSTRACT: *Aiming to observe the dynamic of the degree of polarization during propagation in a noisy channel, we assume a depolarizing channel model for optical fiber. A simulation of the model is performed, showing the decrease of the degree of polarization during channel propagation. Then we implement an experimental set up in order to measure the degree of polarization. The practical results are presented and they can be used to determine the parameter that characterizes the depolarizing channel model.* © 2005 Wiley Periodicals, Inc. Microwave Opt Technol Lett 47: 497–500, 2005; Published online in Wiley InterScience (www.interscience.wiley.com). DOI 10.1002/mop.21210

Key words: *light polarization; depolarizing channel; degree of polarization*

1. INTRODUCTION

Polarization is a very important property of electromagnetic waves that plays a crucial role in optical-communication systems. For example, polarization-mode dispersion limits the transmission rate in gigabit optical networks [1–3] and the interference between two beams is masked if both of them are not fully polarized or do not have the same polarization. Polarization has also been extensively studied because of its use in recent quantum technologies such as quantum teleportation [4] and quantum-key distribution [5–7]. The study of quantum polarization requires quantum versions of the Stokes parameters and degree of polarization [8 and references therein]. However, for single-photon light, as required in some protocols of quantum-key distribution, the mathematical tools commonly used in classical light polarization, coherence matrix, and Stokes parameters [9], can be employed. In fact, all information about a single-photon polarization can be obtained from its coherence matrix J or its Stokes vector S. Therefore, one can explain polarimetric single-photon quantum-key distribution (QKD) using either the Stokes vector or the coherence matrix. In this case, in order to represent the statistical properties correctly, the following condition must be satisfied:

$$s_0 = Tr(J) = 1, \tag{1}$$

where s_0 is the Stokes parameter that indicates the total light power (polarized + unpolarized) and Tr is the trace operation. In the measurement of the polarization of a single-photon pulse on a 2D basis, the two possible results will occur with probabilities as follows:

$$p_1 = \frac{1}{2}[1 + S' \cdot S'_m], \tag{2}$$

$$p_2 = 1 - p_1, \tag{3}$$

where the dot is the scalar product and S' and S'_m are the Stokes vector of the light whose polarization we want to measure S and the Stokes vector of the polarizer S_m, respectively, without their first vector component, s_0 and s_0^m. If the incident light is partially polarized, we have $|S'| < 1$ and $0 < p_1 < 1$; hence, we can never be completely sure about its polarization before the measurement.

The concept of a distinguishability measure between coherence matrices (or Stokes vectors) can be defined based on the same concept used in the distinguishability of probability density functions. Considering coherence matrices and Stokes vectors, the error probability PE is given by

$$PE(S_a, S_b) = \frac{1}{2} - \frac{1}{4}\left|(S'_a - S'_b)\cdot S'_m\right|, \quad (4)$$

$$PE(J_a, J_b) = \frac{1}{2} - \frac{1}{2}\left|Tr[(J_a - J_b)J_m]\right|. \quad (5)$$

If two light beams, represented by the Stokes vectors S_a and S_b, have $s_1^a = s_1^b$, $s_2^a = s_2^b$, and $s_3^a = s_3^b$, then they are indistinguishable, independent of the basis chosen for the measurement. In this case, $(S'_a - S'_b) = 0$ and $PE = 0.5$. If S_a and S_b represent orthogonal polarization states and $S_m = S_a$ or $S_m = S_b$, then $PE = 0$ and the states are maximally distinguishable. Finally, if $S'_a - S'_b$ is orthogonal to S'_m, then $PE = 0.5$ and the states are indistinguishable again. Hence, if the emitter wants to be completely understandable by the receiver, it encodes its messages using orthogonal states on the same basis used in the measurement at the receiver end. In all other cases, there will always be an uncertainty in the message received. Quantum-key distribution uses this fact to protect the bits of the key. In the BB84 protocol [5–7], for each bit of the key, the emitter and the receiver choose, independently and randomly, a polarization state for encoding and the basis for the measurement, respectively, within a restricted and properly chosen set of polarization states. For example, for encoding the bits 0 and 1 in two bases, the emitter can choose one of the polarization states, basis 1: {0(0), π/2(2)} or basis 2: {π/4(0), 3π/4(1)}, while the receiver chooses the rectangular (basis 1) or diagonal (basis 2) basis for the measurement. In this way, for each bit of the key, they randomly choose the distinguishability between the maximum, when $PE = 0$, and the minimum, when $PE = 0.5$. To complete the BB84 protocol, after the transmitter has sent all single-photon pulses to the receiver, they inform to each other, publicly, which basis they have used (but not the results obtained in the receiver's measurement). In the cases where they have used the same basis, PE will be 0 and they keep the bit to form the key. On the other hand, for the cases where they have used different bases, PE will be 0.5 and, since the receiver is not sure of the values of the bits measured, the bits are discarded.

Although PE is a distinguishability measure between J_a (S_a) and J_b (S_b), it is not a distance measure. A distance measure must be equal to 0 when the states are indistinguishable and equal to 1 when the states are maximally distinguishable. One of the most used distance measures is the Kolmogorov distance K, which is related to PE as follows:

$$K(J_0, J_1) = 1 - 2PE(J_0, J_1) = \left|Tr[(J_0 - J_1)J_m]\right| = \frac{1}{2}\left|(S'_0 - S'_1)\cdot S'_m\right| = K(S_0, S_1). \quad (6)$$

Fully polarized states are ideal for quantum communication; however, they are hard to preserve. Indeed, due to interaction with the environment, the fully polarized states become partially polarized or even completely depolarized states. A partially polarized beam can be decomposed in a sum of a completely unpolarized beam and a completely polarized beam, $J = J_{unp} + J_p$, and its degree of polarization (which quantifies how polarized the light is) is defined as being equal to $g_p = Tr(J_p)$ or $g_p = \sqrt{s_1^2 + s_3^2 + s_3^2}$ [9], where the condition (1) is assumed. Hence, a partially polarized state can be written as

$$J = J_{unp} + J_p = (1 - g_p)\frac{I}{2} + g_p\begin{bmatrix}\cos^2(\theta) & \cos(\theta)\sin(\theta)e^{i\phi}\\ \cos(\theta)\sin(\theta)e^{-i\phi} & \sin^2(\theta)\end{bmatrix}, \quad (7)$$

where I is the identity matrix. In the case of single-photon light, the degree of polarization works as a probability. With probability g_p, the polarization state is fully polarized and with probability $(1 - g_p)$, the polarization state is completely depolarized.

As discussed above, for a communication system to work properly, the receiver must be able to distinguish the symbols sent by the sender. Hence, the receiver performs a measurement in the state sent by the emitter and, according to its result, infers which state (symbol) was sent. Let us initially suppose that the following partially polarized states are used for codification of bits 0 and 1, respectively:

$$J_a = (1 - g_p^a)\frac{I}{2} + g_p^a\begin{pmatrix}\cos^2(\theta) & \cos(\theta)\sin(\theta)\\ \cos(\theta)\sin(\theta) & \sin^2(\theta)\end{pmatrix}, \quad (8)$$

$$J_b = (1 - g_p^b)\frac{I}{2} + g_p^b\begin{pmatrix}\cos^2(\varphi) & \cos(\varphi)\sin(\varphi)\\ \cos(\varphi)\sin(\varphi) & \sin^2(\varphi)\end{pmatrix}, \quad (9)$$

where, for simplification, the fully polarized parts of Eqs. (8) and (9) have no complex values. The Kolmogorov distance between those density matrices is given by

$$K = \sqrt{0.25(g_p^b - g_p^a)^2 + g_p^b g_p^a \sin^2(\varphi - \theta)}. \quad (10)$$

For example, the Kolmogorov distance between any pure state ($g_p = 1$) and the completely depolarized state ($g_p = 0$) is 0.5. A nonideal QKD system could employ, for example, the following partially polarized states:

$$J_0 = (1 - g_p^0)\frac{I}{2} + g_p^0\begin{pmatrix}1 & 0\\ 0 & 0\end{pmatrix}, \quad J_{\pi/2} = (1 - g_p^{\pi/2})\frac{I}{2} + g_p^{\pi/2}\begin{pmatrix}0 & 0\\ 0 & 1\end{pmatrix}, \quad (11)$$

$$J_{\pi/4} = (1 - g_p^{\pi/4})\frac{I}{2} + g_p^{\pi/4}\begin{pmatrix}1/2 & 1/2\\ 1/2 & 1/2\end{pmatrix}, \quad J_{3\pi/4} = (1 - g_p^{3\pi/4})\frac{I}{2} + g_p^{3\pi/4}\begin{pmatrix}1/2 & -1/2\\ -1/2 & 1/2\end{pmatrix}, \quad (12)$$

and the Kolmorogov distances between them are given by

$$K(J_i, J_j) = \begin{cases}\dfrac{g_p^i + g_p^j}{2}, & \text{if } i = j \pm \pi/2\\ \dfrac{\sqrt{(g_p^i)^2 + (g_p^i)^2}}{2}, & \text{if } i = j \pm \pi/4, \pm 3\pi/4\end{cases}. \quad (13)$$

Hence, if polarization states (11) and (12) are used in QKD, an error rate will exist between the transmitter and receiver, given by

$E = 0.5 - 0.125(g_p^0 + g_p^{\pi/2} + g_p^{\pi/4} + g_p^{3\pi/4})$. Thus, as is already well known, the unpolarized part of the states introduces an uncertainty in the communication, thus increasing the error rate.

2. DYNAMIC OF POLARIZATION IN A DEPOLARIZING CHANNEL

As explained in the Introduction, the quantum communication protocols work well for fully polarized light; however, when a fully polarized light propagates in a common optical fiber, the light experiments several random rotations in its polarization due to random birefringence in the fiber that can be produced, for example, by mechanical stress like bending, impurities during the fabrication process, and noncircularity of the core. Hence, it is important to discuss and measure the depolarizing effect during light propagation. When the fiber properties do not vary, the optical fiber can be modeled by a unitary matrix called the Jones matrix T_F, given by [9]:

$$T_F = C_\delta R_\theta C_\xi = \begin{bmatrix} \cos(\theta)\exp[i(\xi+\delta)/2] & -\sin(\theta)\exp[-i(\xi-\delta)/2] \\ \sin(\theta)\exp[i(\xi-\delta)/2] & \cos(\theta)\exp[-i(\xi+\delta)/2] \end{bmatrix}, \quad (14)$$

$$C_\alpha = \begin{bmatrix} \exp(i\alpha/2) & 0 \\ 0 & \exp(-i\alpha/2) \end{bmatrix}; \quad R_\theta = \begin{bmatrix} \cos(\theta) & -\sin(\theta) \\ \sin(\theta) & \cos(\theta) \end{bmatrix}, \quad (15)$$

where C is a compensator ($\lambda/4$ plate) and R is a rotator ($\lambda/2$ plate). If the fiber birefringence varies randomly, the fiber is seen as a noisy channel that is modeled taking into consideration that the fiber can be represented by different values of T_F, with each one of them having an associated probability. So, if J_i is the coherence matrix of the light at the input of the noisy channel modeled by the set $\{p_k, T_{Fk}\}_{k=1}^n$, the coherence matrix of the light at the fiber output, J_o, is given by

$$J_o = \sum_{k=1}^{n} p_k T_{Fk} J_i T_{Fk}^{+}, \quad (16)$$

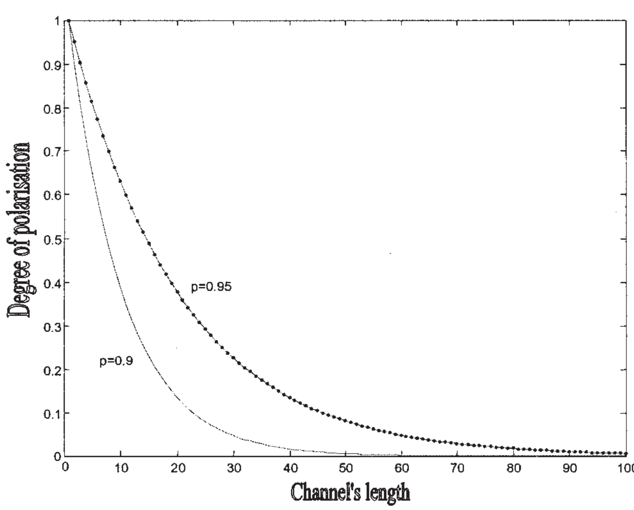

Figure 1 Dynamic of the degree of polarization when an optical beam, initially fully polarized, propagates in a depolarizing channel having $p = 0.95$ (line-dot) and $p = 0.9$ (line)

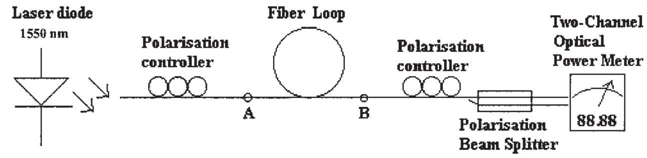

Figure 2 Optical setup for polarization degree measurement

where the upper index "+" denotes the conjugated and transposed matrix. In order to model our fiber, we chose the depolarizing channel. This channel, with probability p, allowed the input polarization state to remain intact, while, with probability $(1 - p)$, the output state became completely unpolarized. Thus, the channel's model and the output coherence matrix are respectively given by

$$\{p, T_F\} = \{((3p+1)/4; I), (p/4; X), (p/4; Y), (p/4; Z)\}, \quad (17)$$

$$X = C_\pi R_{\pi/2} C_0 = i\begin{bmatrix} 0 & 1 \\ 1 & 0 \end{bmatrix}; \quad Y = C_0 R_{\pi/2} C_0 = -i\begin{bmatrix} 0 & -i \\ i & 0 \end{bmatrix}; \quad Z = C_{\pi/2} R_0 C_{\pi/2} = i\begin{bmatrix} 1 & 0 \\ 0 & -1 \end{bmatrix},$$

$$J_o = pIJ_iI + (1-p)\left[\frac{IJ_iI + XJ_iX + YJ_iY + ZJ_iZ}{4}\right] = (1-p)I/2 + pJ_i. \quad (18)$$

Comparing Eqs. (18) and (7), we see that the polarization degree of the output state is exactly equal to the channel's probability p. In order to follow the decrease of the degree of polarization during noisy channel propagation, we shared the optical fiber in 100 small pieces and modeled each piece by Eqs. (17)–(18), using $p = 0.9$ (case 1) and $p = 0.95$ (case 2). The simulation of the channel propagation is shown in Figure 1. Obviously, the lower the probability p, the faster the degree of polarization tends to zero.

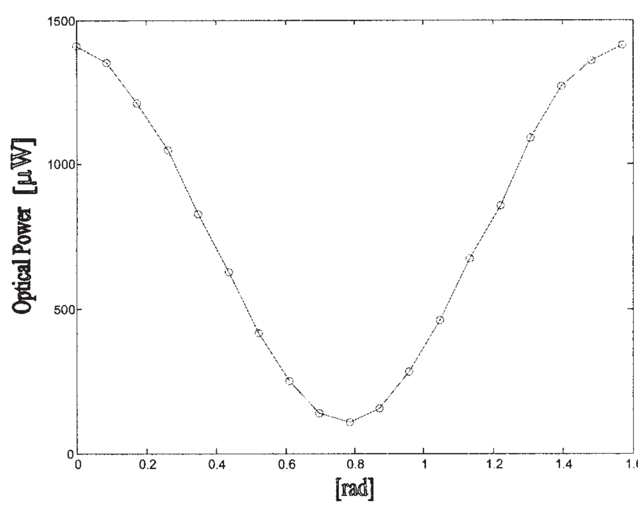

Figure 3 Variation of the optical power at the polarizer beam splitter's output vs. variation of the $\lambda/2$ plate of the second polarization controller without noisy channel

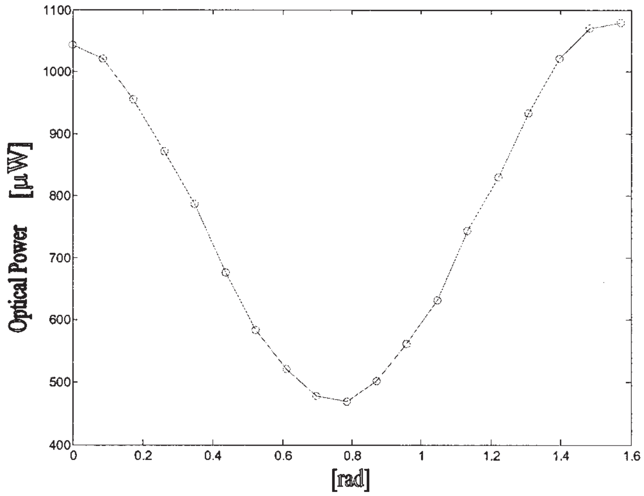

Figure 4 Variation of the optical power at the polarizer beam splitter's output vs. variation of the λ/2 plate of the second polarization controller with noisy channel (200-m optical-fiber coil) introduced

3. EXPERIMENTAL RESULTS OF THE MEASUREMENT OF THE DEGREE OF POLARIZATION WITH CW INPUT LIGHT

In order to measure the degree of polarization, we used the setup shown in Figure 2. In this figure, the light source is the CW laser diode CQF915/108 operating in 1550.91 nm. The first polarization controller (PC) defines the polarization state that will be used. This state is the same that gives the maximal optical power, in the absence of the fiber loop and the second polarization controller, at the upper polarization beam splitter (PBS) output (and minimal at the other output), that is, we matched the input polarization state with the polarization state that characterizes the PBS. Then we introduced the second PC and the points A and B were still together. The second PC has its λ/4 plates adjusted initially, in order to give the maximal optical power at the upper PBS output, then the λ/2 plate was varied and the variation of the optical power measured at the upper PBS output is shown in Figure 3. The degree of polarization is given by

$$g_p = \frac{P_{\max} - P_{\min}}{P_{\max} + P_{\min}}, \tag{19}$$

where $P_{\max}$ and $P_{\min}$ are, respectively, the maximal and minimal values found in Figure 3. The value for the degree of polarization obtained is $g_p = 0.859$. Now, we use a 200-m optical-fiber coil as a noisy channel. The same procedure as before is realized and the variation of the optical power at the upper PBS output is shown in Figure 4. In this figure, we can clearly see the effect of the decrease of the degree of polarization in the distinguishability between the maximal and minimal values of the power. For the second experiment, the value of the degree of polarization is $g_p = 0.394$. At last, using the channel model presented in Eqs. (17)–(18) and the g_p value measured, we conclude that, for the 200-m fiber coil, $p = 0.394$. Although the results have been obtained using multiphoton pulses, the g_p value obtained is the same that we would obtain if we had used a single-photon source and a single-photon detector and had measured the probability of detection in the upper PBS arm, instead of the optical power.

4. CONCLUSION

Initially, we described the theory of single-photon polarization and the BB84 quantum-key distribution (QKD) protocol using classical tools: the Stokes' parameters and the coherence matrix. Then, aiming to observe the dynamic of the degree of polarization during propagation in a noisy channel, we assumed the depolarizing channel model for optical fiber. A simulation was performed, showing the decrease of the degree of polarization during channel propagation. Lastly, we implemented an experimental setup in order to measure the degree of polarization. The practical results were presented and they can be used to determine the parameter *p* of the depolarizing channel model.

ACKNOWLEDGMENT

This work was supported by the Brazilian agency CNPq.

REFERENCES

1. S.J. Savory and F.P. Payne, Pulse propagation in fibers with polarization-mode dispersion, J Lightwave Technol 19 (2001), 350.
2. G.D. VanWiggeren and R. Roy, Transmission of linearly polarized light through a single-mode fiber with random fluctuations of birefringence, Applied Optics 38 (1999), 3888.
3. D. Mahgerefteh and C.R. Menyuk, Effect of first-order PMD compensation on the statistics of pulse broadening in a fiber with randomly varying birefringence, IEEE Photon Technol Lett 11 (1999), 340.
4. C.H. Bennett, G. Brassard, C. Crépeau, R. Jozsa, A. Peres, and W.K. Wootters, Teleporting an unknow quantum state via dual classical and Einstein–Podolsky–Rosen channels, Phys Rev Lett 70 (1993), 1895.
5. J. Breguet, A. Muller, and N. Gisin, Quantum cryptography with polarized photons in optical fibers: Experimental and practical limits, J Modem Optics 41 (1994), 2405.
6. J. Breguet, A. Muller, and N. Gisin, Experimental demonstration of quantum cryptography using polarized photons in optical fiber over more than 1 km, Europhys Lett (1993), 383.
7. J.D. Frasson and H. Ilves, Quantum cryptography using optical fibers, Appl Optics 33 (1994), 2949.
8. A. Luis, Quantum degree of polarization, Phys Rev A 66 (2002), 13806.
9. M. Born and E. Wolf, Principles of optics, 7th ed., Cambridge University Press, Cambridge, 1999.

A BROADBAND SEMICIRCLE PROBE-FED PENTAGON-SLOT MICROSTRIP PATCH ANTENNA

Irene Ang and B. L. Ooi
National University of Singapore
10 Kent Ridge Crescent
Singapore 119260

Received 26 May 2005

ABSTRACT: *A wideband pentagon-slot microstrip antenna with a semicircle probe feed is proposed. The broadband characteristic is achieved by cutting a pentagon slot at each corners of the patch. The proposed antenna is able to achieve an impedance bandwidth of 68.3% for a VSWR of less than 2. Experimental comparison with a similar-size retangular microstrip patch antenna has also been conducted in this paper.* © 2005 Wiley Periodicals, Inc. Microwave Opt Technol Lett 47: 500–505, 2005; Published online in Wiley InterScience (www.interscience.wiley.com). DOI 10.1002/mop.21211

Key words: *patch antenna; probe-fed antenna; broadband antenna*

1. INTRODUCTION

Microstrip antennas have been widely used due to their advantages such as light weight and small size. However, it is well known that